

Supporting Information

© Wiley-VCH 2012

69451 Weinheim, Germany

**Aptamer-Functionalized, Ultra-Small, Monodisperse Silica  
Nanoconjugates for Targeted Dual-Modal Imaging of Lymph Nodes  
with Metastatic Tumors\*\***

*Li Tang, Xujuan Yang, Lawrence W. Dobrucki, Isthier Chaudhury, Qian Yin, Catherine Yao,  
Stéphane Lezmi, William G. Helferich,\* Timothy M. Fan,\* and Jianjun Cheng\**

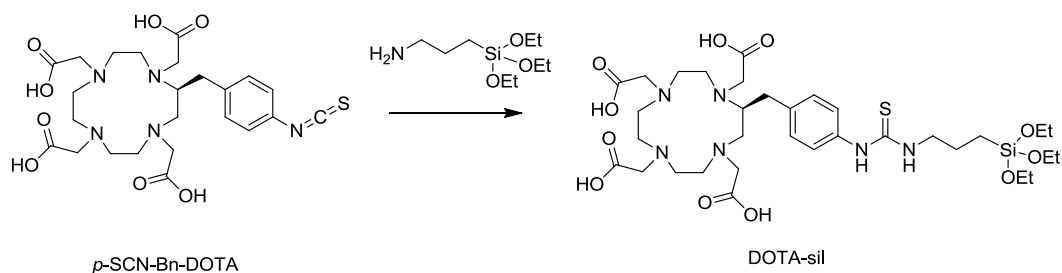
anie\_201205271\_sm\_miscellaneous\_information.pdf  
anie\_201205271\_sm\_movie\_s1.mpg

## General

All chemicals including tetraethyl orthosilicate (TEOS, 99.999%) were purchased from Sigma-Aldrich (St Louis, MO, USA) unless otherwise noted. (S)-2,2',2'',2'''-(2-(4-isothiocyanatobenzyl)-1,4,7,10-tetraazacyclododecane-1,4,7,10-tetrayl)tetraacetic acid (*p*-SCN-Bn-DOTA) was purchased from Macrocyclics, Inc. (Dallas, TX, USA). mPEG<sub>5k</sub>-triethoxysilane (PEG-sil) (Scheme 1) and maleimide-PEG<sub>5k</sub>-SCM (MAL-PEG-NHS) were purchased from Laysan Bio (Arab, AL, USA). All oligonucleotides used in this study were purchased from Integrated DNA Technologies Inc. (Coralville, IA, USA) with following sequences: nucleolin aptamer (NCL-Apt): 5'-GGT GGT GGT GGT TGT GGT GGT GGT GGT TTT TTT TTT TTT TTT TT/3ThioMC3-D/-3'; the control DNA: 5'-GAG AAC CTG AGT CAG TAT TGC GGA GAT TTT TTT TTT TT/3ThioMC3-D/-3'. DNA concentration was measured on NanoDrop 2000 (Thermo Scientific, Wilmington, DE, USA). All chemicals and DNAs were used as received unless otherwise noted. Anhydrous solvents were obtained by passing HPLC-grade regular solvent through dry alumina columns and stored with molecular sieves in a glovebox. Rhodamine B isothiocyanate (RITC)- or IR783-containing silanes were prepared as described previously.<sup>[1]</sup> The sizes and monodispersities of silica nanoparticles were determined with a Hitachi S4800 high resolution Scanning Electron Microscope (SEM). The  $\zeta$ -potential of particles was measured on a Malvern Zetasizer Nano-ZS with a 633 nm laser (Malvern Instruments Ltd., Worcestershire, UK). Measurement of fluorescence spectra of silica nanoparticles was carried out on a LS55 fluorescence spectrometer (Perkin Elmer, Santa Clara, CA, USA). Murine 4T1 cells engineered with firefly luciferase were provided by Dr. David Piwnica-Worms from Washington University (St. Louis, MO, USA). Cells were cultured in DMEM medium containing 10% Fetal Bovine Serum (FBS), 100 units/mL aqueous penicillin G and 100  $\mu$ g/mL streptomycin (Invitrogen, Carlsbad, CA, USA) at 37°C in 5% CO<sub>2</sub> humidified air. Cells were harvested at 80% confluence with EDTA/trypsin, counted and re-suspended for experiments. The flow cytometry analysis of cells was conducted with a BD FACSCanto 6 color flow cytometry analyzer (BD, Franklin Lakes, NJ, USA). Female C57BL/6 or BABL/c mice were purchased from National Cancer Institute (NCI, Frederick, MD, USA). Feed and water were available *ad libitum*. Artificial light was provided in a 12/12 hour cycle. The study protocol was reviewed and approved by the Illinois Institutional Animal Care and Use Committee (IACUC) of

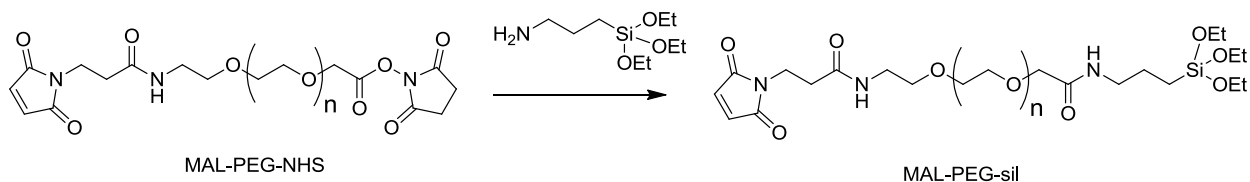
University of Illinois at Urbana–Champaign. Micro-PET/CT imaging was performed with small animal on a Siemens Inveon PET-CT system (Siemens Healthcare, USA). *Ex vivo* measurement of the radioactivity was conducted on a 2480 Wizard2 Automatic Gamma Counter (Perkin-Elmer). The fluorescence intensity in the extracted lymph node was measured *ex vivo* at  $\lambda_{em}=800$  nm with Odyssey infrared mouse imaging system (LI-COR, Lincoln, NE, USA). The flash frozen lymph node tissue was embedded with optimum cutting temperature (O.C.T.) compound (Sakura Finetek USA, Torrance, CA, USA), sectioned by a Leica CM3050S cryostat and mounted on glass slides for histological analysis.

### Synthesis of 1,4,7,10-Tetraazacyclododecane-1,4,7,10-Tetraacetic Acid (DOTA) Containing Silane (DOTA-sil, Scheme 1)



To a reaction vial containing 3-aminopropyltriethoxysilane (4.8 mg, 0.022 mmol) was added an anhydrous dimethylformamide (DMF) solution (0.5 mL) of DOTA-NCS (10 mg, 0.018 mmol) and triethylamine (3.6 mg, 0.036 mmol). The reaction mixture was stirred for 4 h under nitrogen protection at rt. The solvent and triethylamine were removed under vacuum to give DOTA-sil, which was used directly without further purification.

### Synthesis of Maleimide-PEG<sub>5k</sub> Containing Silane (MAL-PEG-sil, Scheme 1)



In a reaction vial containing 3-aminopropyltrimethoxysilane (4.4 mg, 0.020 mmol) was added an anhydrous DMF solution (1 mL) of MAL-PEG-NHS (17 mg, 0.004 mmol) and triethylamine (2.0 mg, 0.02 mmol). The reaction mixture was stirred for 4 h under nitrogen at rt. The solvent and triethylamine were removed under vacuum to give MAL-PEG-sil, which was used directly without further purification.

### **General Procedures for the Preparation of Dual-Mode Silica Nanoconjugates (NCs)**

The size-controlled, dual-mode silica NCs were prepared similarly as previously reported.<sup>[1]</sup> The size of NC was controlled by the reaction condition (Table S1). For example, to prepare the NC200, methanol (1.0 mL), DI water (0.27 mL) and concentrated ammonia (0.24 mL) were mixed. TEOS (62.5  $\mu$ L, 0.28 mmol) was then added to the solvent mixture and stirred for 10 min followed by the addition of a methanol solution (100  $\mu$ L) of NIR-sil (2 mg, 2.2  $\mu$ mol). The mixture was stirred at a stirring rate of 100 rpm at rt in dark for 12 h to form the fluorescent core of the NC. Next, a methanol solution (200  $\mu$ L) of DOTA-sil (2 mg, 2.6  $\mu$ mol) was added to the reaction mixture and stirred for 10 min followed by the addition of PEG-sil (20 mg/mL, 100  $\mu$ L) to modify the surface of NC. The mixture was further stirred for 6 h at the same stirring speed. The resulting NCs were collected by centrifugation at 15k rpm, washed by ethanol ( $3 \times 1$  mL) and redispersed in DI water or PBS (1 $\times$ ) before use. To characterize the size of NCs, one drop of a dilute solution of NCs in ethanol on a silicon wafer was allowed to dry in air and then analyzed by SEM at 5 kV. The diameter of NC was determined by measuring 100 particles on representative SEM images and averaging their sizes. NCs with other sizes were similarly prepared, but by using different concentrations of TEOS, water and ammonia (Table S1).

### **Surface Conjugation with DNA**

To conjugate the DNA to the NC surface, size controlled NCs were prepared similarly as described above except for that the surface of NCs were modified by MAL-PEG-sil (20 mg/mL, 100  $\mu$ L) (Scheme 1). The sequence of the NCL-Apt is 5'-GGT GGT GGT GGT TGT GGT GGT GGT GGT TTT TTT TTT TTT TTT TT/3ThioMC3-D/-3'. Poly-T sequence was employed as a spacer to allow the recognition sequence to fully extend from the NC surface for the most efficient targeting. For example, to conjugate the NC20 with NCL-Apt, NCL-Apt (5 nmol) in

100  $\mu$ L PBS (1 $\times$ ) was first mixed with tris(2-carboxyethyl)phosphine (100 nmol) and stirred for 2h at rt to reduce the disulfate bond at the 3'-end of DNA to give NCL-Apt with a free thiol group for conjugation. The reduced NCL-Apt (5 nmol, without further purification) was then added to the NC (5 mg, surface modified by MAL-PEG-sil) in 250  $\mu$ L PBS (1 $\times$ ). The mixture was stirred overnight at rt. The resulting NCs were collected by centrifugation at 15k rpm, washed by PBS (1 $\times$ ) (3  $\times$  1 mL) and redispersed in PBS (1 $\times$ ) before use. To determine the conjugation efficiency, the NCs were centrifuged at 15k rpm. The DNA concentration in the supernatant was monitored with NanoDrop 2000 before and after the conjugation. The size of NC was characterized with SEM and DLS as described above. The conjugation of Ctrl-DNA to the surface of NCs followed the procedure described above. RITC labeled NC20-Ctrl and NC20-Apt were prepared similarly as described previously.<sup>[1]</sup>

### **Measurement of $\xi$ -Potential**

The  $\xi$ -potential of the NCs was determined on a Malvern zetasizer by using freshly prepared NC solution at a concentration of 0.5 mg/mL in DI water.

### **<sup>64</sup>Cu Labeling of NCs**

The <sup>64</sup>Cu chloride (obtained from the Washington University, St. Louis, MO, USA) was mixed with silica NC (2 mg) in a NH<sub>4</sub>OAc buffer solution (pH = 5.5, 0.1 M, 0.3 mL) (Figure S1). The mixture was incubated for 1 h at 80°C. To determine the labeling efficiency, the NCs were spun down (15k rpm, 5 min) and the radioactivity in the supernatant and the precipitation was measured respectively. The <sup>64</sup>Cu-labeled silica NCs were purified by centrifugation and washed by PBS (1 $\times$ ) once (1 mL). The purified <sup>64</sup>Cu-labeled silica NCs were then re-suspended in PBS (1 $\times$ ) for the animal study.

### **Stability of <sup>64</sup>Cu Labeling in Serum**

The <sup>64</sup>Cu-labeled NCs was dispersed in 50% reconstituted human serum (Sigma-Aldrich, 0.6 mg/mL), equally distributed to 9 vials with 0.1 mL NC solution per vial, and then incubated at 37°C. At selected time intervals (0, 3, and 6 h), three selected vials of each group were taken out of the incubator. The NC solution was centrifuged at 14k rpm for 5 min and the supernatant was

transferred to a nonradioactive tube for radioactivity measurement on a  $\gamma$ -counter to determine the amount of disassociated  $^{64}\text{Cu}$ .

### **Cellular Internalization of NCs**

To examine cell uptake of Apt functionalized silica NC, NC20-Apt and NC20-Ctrl labeled with RITC were prepared as described previously.<sup>[1]</sup> 4T1 cells ( $2 \times 10^5$ ) were seeded in a 12-well plate for 24 h. RITC labeled NC20-Apt and NC20-Ctrl (100  $\mu\text{mL}$ ) were incubated with the cells in opti-MEM (1 mL) for 2 h (37 °C). The cells were then washed with PBS (1 mL  $\times$  3) and detached *via* trypsinization. Cells were fixed with 4% paraformaldehyde for flow cytometry analysis ( $1 \times 10^4$  cells analyzed, PE-A channel). Both the percentage of the fluorescent cells relative to the total analyzed cells and the mean fluorescence intensity of the total cells were assessed. All experiments were performed in triplicate.

### **Micro-PET/CT Imaging**

Fifteen minutes before the imaging experiment, mice were anesthetized by isoflurane (~2%) in an induction chamber.  $^{64}\text{Cu}$ -labeled NCs (~30  $\mu\text{Ci}$ , 20  $\mu\text{L}$ ) were given via hock injection. Mice were placed on the micro-CT imaging bed and kept anaesthetised with a constant isoflurane flow. A dynamic PET scan was acquired for 1 h (60 min acquisition time, reconstructed as 60 frames at 60 seconds/frame). The micro-CT scan (80keV/500uA X-rays energy, 360 projections, 360 degrees, 75  $\mu\text{m}$  pixel size) was used for determining the anatomical localization of LNs. Static micro-PET scans were acquired at two selected time points (6 and 24 h p.i.) together with micro-CT scans for anatomical co-registration. The obtained micro-PET and micro-CT images were reconstructed using ordered subset expectation maximization (OSEM) and cone-beam algorithms with existing commercial software (Inveon Acquisition Workspace and Cobra Exxim, respectively). Micro-PET images were processed using 3-D median filtering and fused with micro-CT images. To quantify the radioactivity of  $^{64}\text{Cu}$  in LNs, complex irregular volumes of interest (VOIs) were drawn on the micro-CT images and registered with the micro-PET images to determine mean counts in each VOI. To minimize partial volume effects, the anatomical borders of the organs were not included. The radiotracer activity from each VOI was normalized by injected dose and expressed as percent of the decay-corrected injected activity per  $\text{cm}^3$  of

tissue, which can be approximated as percentage %I.D./g assuming the density of tissue is  $\sim 1 \text{ g/cm}^3$ . The initial total injected activity was determined by dose calibrator before the injection.

### **Radioactivity measurement with $\gamma$ -counter**

Mice were euthanized and dissected after the final micro-PET/CT imaging session (24 h p.i.). The LNs at both sides were collected, weighed and measured for the  $^{64}\text{Cu}$  radioactivity with a Wizard2 automatic  $\gamma$ -counter using appropriate energy window at photopeak of 511 keV. Raw counts were corrected for background, decay, and weight. Corrected counts were converted to microcurie ( $\mu\text{Ci}$ ) per gram by using a previously determined calibration curve with  $^{64}\text{Cu}$  standards. The radioactivity in each collected tissue sample was calculated as percentage of injected dose per gram of tissue (%I.D./g). For this calculation, the radioactivity in tissue was corrected for decay to the time of  $\gamma$ -well counting.

### **Fluorescence Imaging**

Mice were euthanized and dissected after all the imaging experiments (24 h p.i.). The I-LNs at both sides were collected, weighed and then fixed in 10% formalin. The I-LNs were imaged on an Odyssey infrared mouse imaging system *ex vivo*. The fluorescence intensity of NIR labeled NCs in the extracted LN was measured at  $\lambda_{\text{em}}=800 \text{ nm}$  (shown as green color) and quantified by the provided software. Autofluorescence from the tissues at  $\lambda_{\text{em}}=700 \text{ nm}$  was shown in red color. The overlay images were shown in Figure 3b.

### **Metastatic LN Tumor Model**

The tumor model was established in 10 week-old female BABL/c mice by subcutaneous injection of  $1 \times 10^5$  of firefly luciferase encoded 4T1 cells to the hock of both rare legs of mice.<sup>[2,</sup>  
<sup>3]</sup> Tumor progression was evaluated using a bioluminescence imaging (BLI) system (Stanford Photonics, Palo Alto, CA) with a dual micro-channel plate ICCD camera. Each mouse was intraperitoneally injected with a D-luciferin potassium salt solution (0.15 g/kg body weight) 3 minutes prior to imaging and then anesthetized with a constant flow of isoflurane-containing oxygen. A grey-scale image of the mouse was first recorded with dimmed light. Photon emission was then integrated for 10 seconds using the imaging software Piper Control (Stanford

Photonics, Palo Alto, CA) and visualized in pseudo-color. To localize bioluminescent signals that indicated luciferase-engineered 4T1 tumors, grey-scale images of mouse body and bioluminescent signals of metastatic tumors were merged using ImageJ (NIH) and Photoshop Elements (Adobe, San Jose, CA). At the end of the study, popliteal LNs from each mouse were excised and cryo-stored for sectioning. Sectioned LN tissues (10  $\mu\text{m}$ ) were stained with hematoxylin and eosin and then observed under an AxioSkop 40 microscope for histological analysis.

### **Statistical Analyses**

Student's *t*-test comparisons with at least 95% confidence interval were used for statistical analysis. The results were deemed significant at  $0.01 < *p \leq 0.05$ , highly significant at  $0.001 < **p \leq 0.01$ , and extremely significant at  $***p \leq 0.001$ .



## Supplementary Figures and Tables

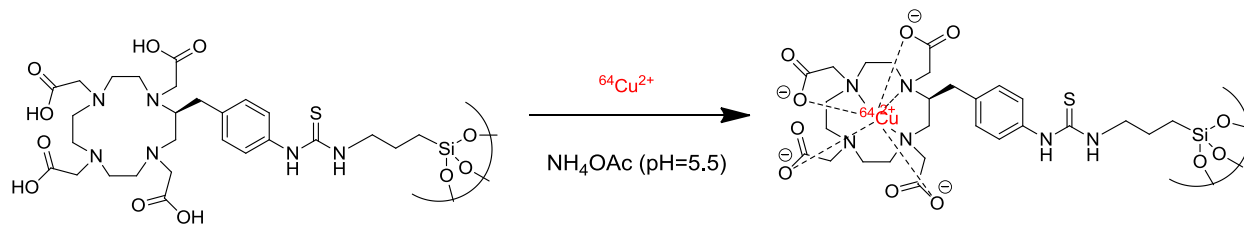


**Figure S1.**  $^{64}\text{Cu}$  labeling of silica NCs.

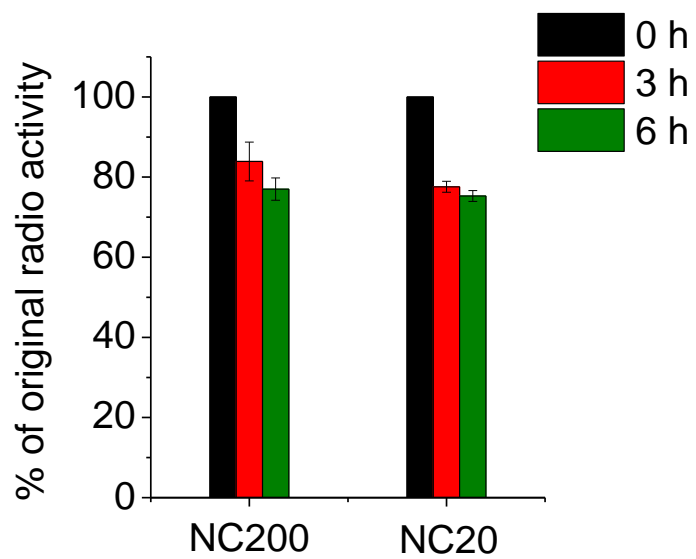


**Figure S2.** Stability of <sup>64</sup>Cu labeling with dual-mode silica NCs in serum.

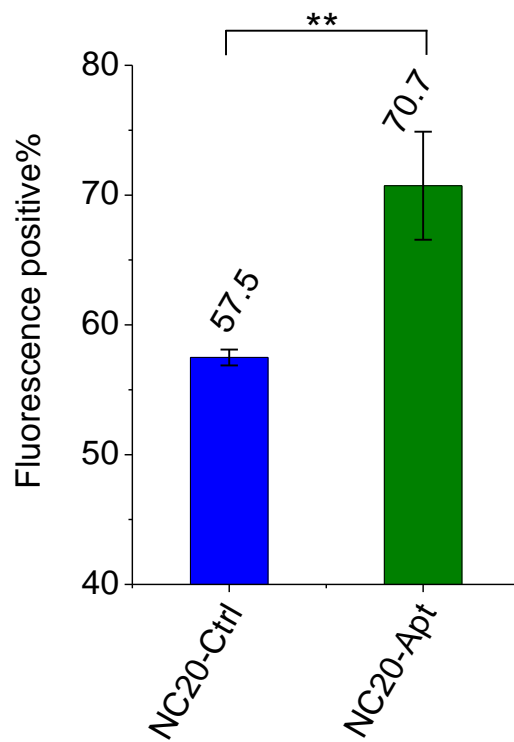


**Figure S3.** *In vitro* 4T1 cell targeting by NC20-Apt. Internalization of NC20-Ctrl and NC20-Apt in 4T1 cells over an 2-h incubation time at 37 °C was evaluated by the percentage of cells containing internalized NCs using flow cytometry.

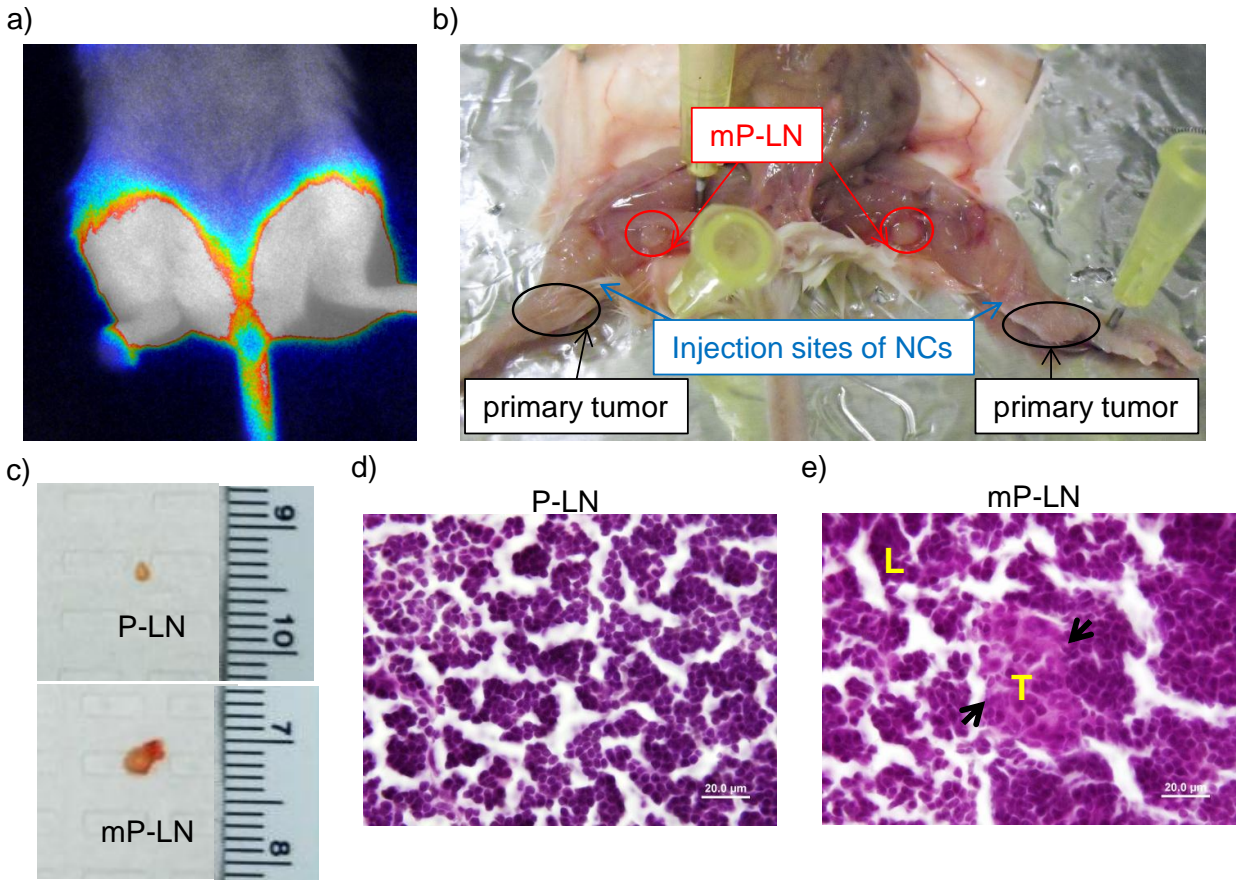


**Figure S4.** a) Bioluminescence image of the BALB/c mice with subcutaneous 4T1 primary tumors (hocks) and mP-LNs. Strong localized bioluminescent signal at injection sites were detected. However, the bioluminescent signal from the mP-LNs cannot be differentiated from that of the primary tumor due to the high intensity; b) Autopsy of the mice with mP-LNs (indicated by red circles and arrows). Primary tumors (black circles and arrows) and injection sites (blue circles and arrows) were also indicated; c) images of excised LNs (mP-LN and normal P-LN); Histology analysis of d) normal P-LNs and e) mP-LNs. Representative sections of LN stained by hematoxylin and eosin were shown. The tumor nodules are indicated by arrows. T: tumor; L: lymph node. Scale bar = 20  $\mu$ m.

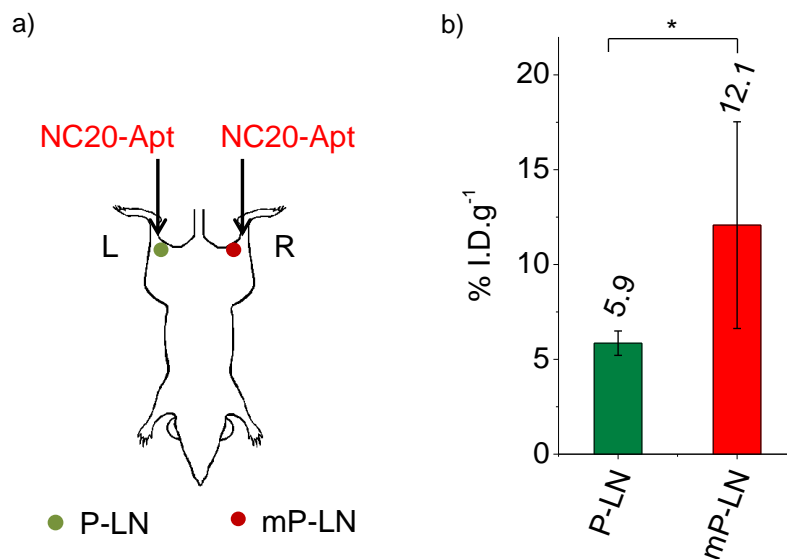


**Figure S5.** a) Dual labeled NC20-Apt was s.c. administered to both sides of the hocks of BABL/c mice. The left P-LN was normal, while the right one was with metastatic tumors (indicated as mP-LN); b) The quantitative analysis of the accumulation of the  $^{64}\text{Cu}$ -labelled NCs was confirmed by *ex vivo* measurement of excised P-LN and mP-LN by  $\gamma$ -counter (average  $\pm$  SD; n=3; \* $p$ <0.05).

**Table S1. Reaction Conditions for Synthesizing Size-Controlled NCs via Stöber Method**

Method	MeOH (mL)	DI water ( $\mu\text{L}$ )	$\text{NH}_4\text{OH}$ ( $\mu\text{L}$ )	TEOS ( $\mu\text{L}$ )
NC20	1.0	360	70	31.2
NC200	1.0	270	240	62.5

**Movie S1** A corresponding 3D renderings of PET/CT image showed the enhanced accumulation of NC20 in the left P-LN and limited accumulation of NC200 in the right P-LN. Dual labeled NC20 (left) and NC200 (right) was administered to C57BL/6 mice through hock injection. The PET/CT image was taken 6 h p.i.. The reconstructed 3D image was rotated along the z-axis as shown in the movie.

## References

- [1] L. Tang, T. M. Fan, L. B. Borst, J. Cheng, *ACS Nano* **2012**, *6*, 3954.
- [2] F. Zhang, G. Niu, X. Lin, O. Jacobson, Y. Ma, H. Eden, Y. He, G. Lu, X. Chen, *Amino Acids* **2012**, *42*, 2343.
- [3] X. L. Huang, F. Zhang, S. Lee, M. Swierczewska, D. O. Kiesewetter, L. X. Lang, G. F. Zhang, L. Zhu, H. K. Gao, H. S. Choi, G. Niu, X. Y. Chen, *Biomaterials* **2012**, *33*, 4370.